

Star formation news letter

276 11-15本目

- 大橋聰史

Resolving the HD 100546 Protoplanetary System with the Gemini Planet Imager: Evidence for Multiple Forming, Accreting Planets

Thayne Currie¹, Ryan Cloutier^{2,8,9}, Sean Brittian³, Carol Grady^{4,10}, Adam Burrows⁵, Takayuki Muto⁶, Scott J. Kenyon⁷, Marc J. Kuchner⁴

Accepted by ApJL

<http://arxiv.org/pdf/1511.02526>

Gemini Planet Imager H bandによる観測

HD 100546 bのガス惑星候補天体を直接撮像 (1-10Mj)

また14AUに10-20Mj candidateを発見

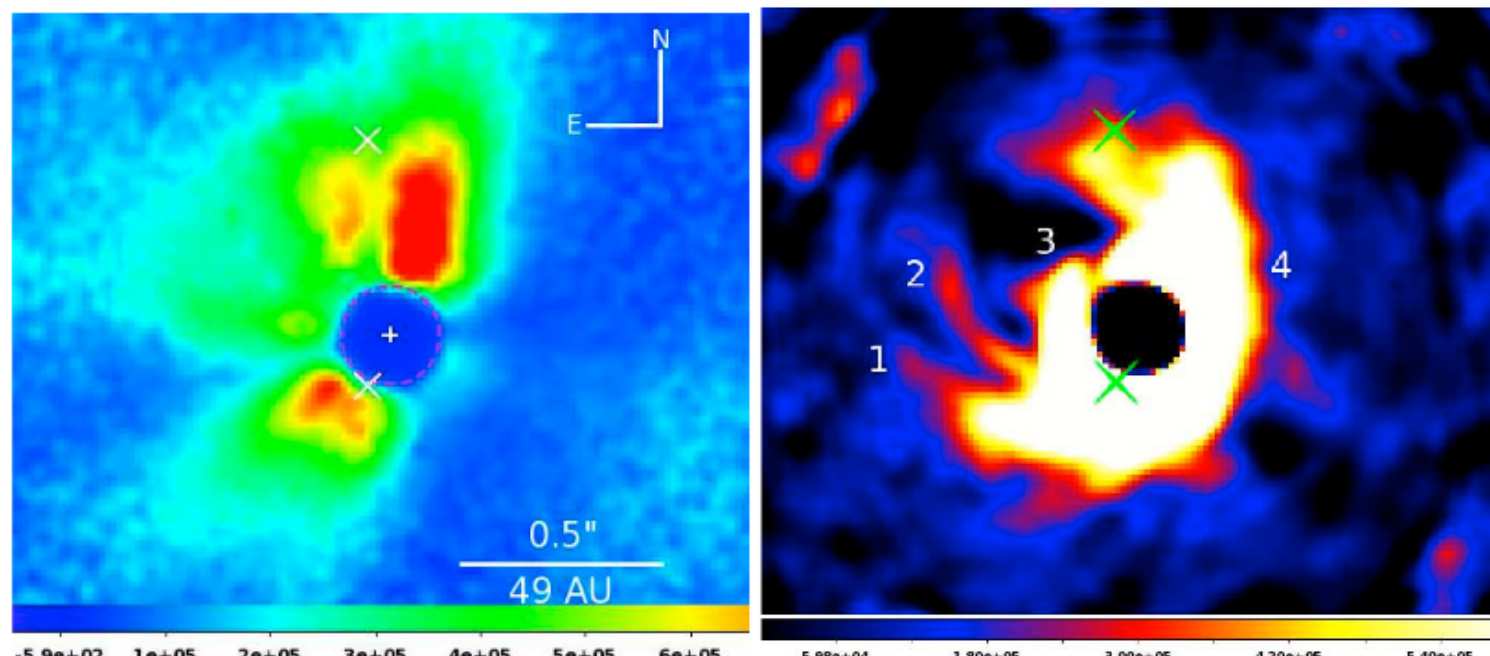
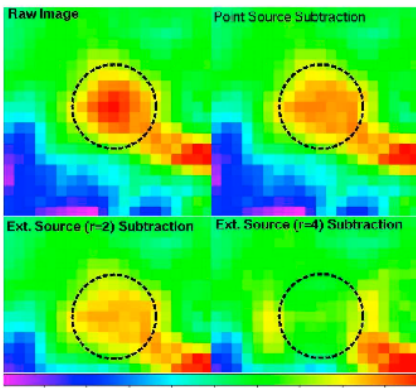
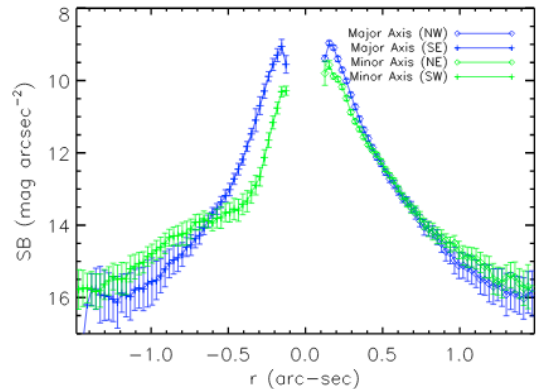


FIG. 1.— HD 100546 stellocentric distance-scaled disk images; an *x* denotes the positions of HD 100546 b and the candidate “HD 100546 c”. (left) Polarized intensity image, showing the inner working angle (magenta dashed line) and the star’s position (cross). The polarized intensity drops interior to $0''.15 - 0''.2$. The dark blue regions the west of the visible disk identify the dark lane (Grady et al [2001], [2005]). (right) Spatially-filtered, wavelength collapsed IFS image, showing the thermal IR bright spiral-like feature (1), a second spiral (2), the position of the proposed spiral identified by Avenhaus et al (2014) (3), and the western rim of the visible disk (4).

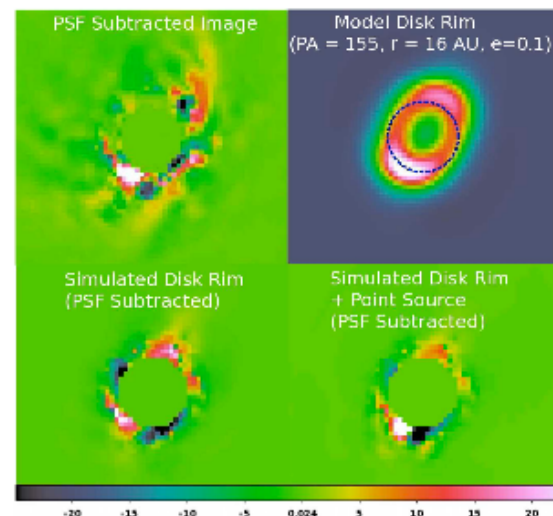
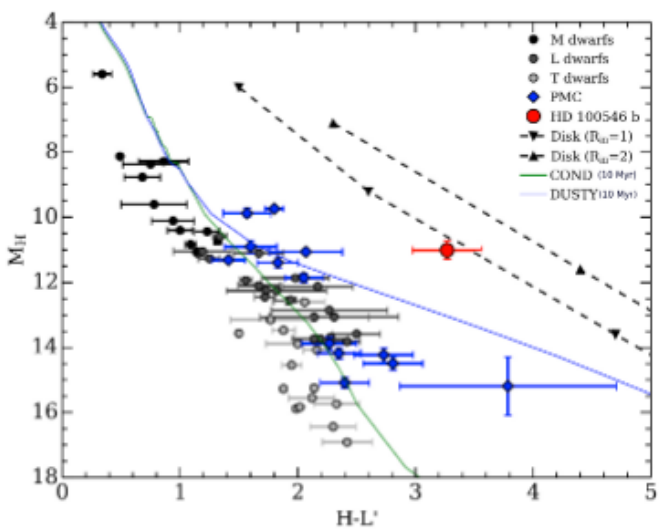
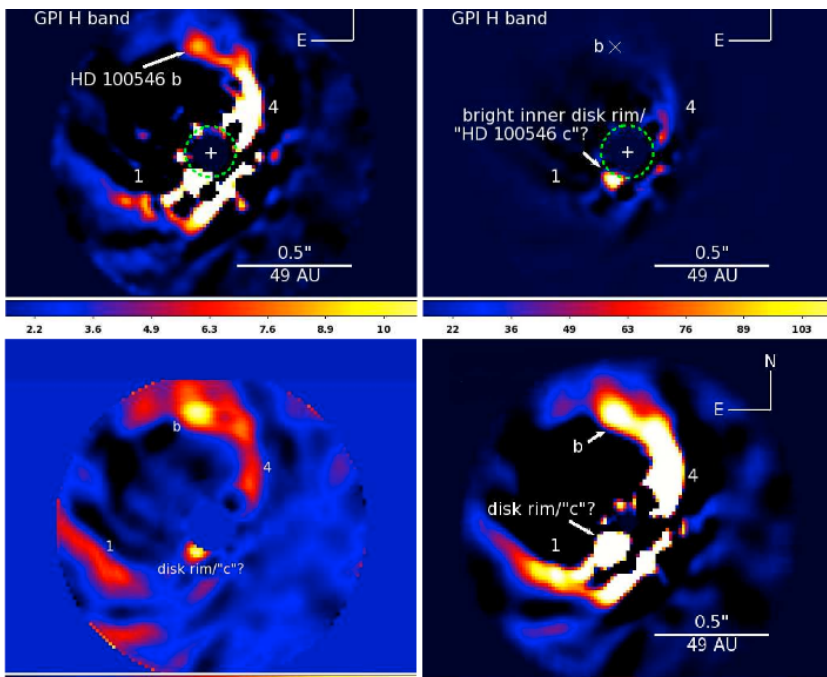
Resolving the HD 100546 Protoplanetary System with the Gemini Planet Imager: Evidence for Multiple Forming, Accreting Planets

Thayne Currie¹, Ryan Cloutier^{2,8,9}, Sean Brittian³, Carol Grady^{4,10}, Adam Burrows⁵, Takayuki Muto⁶, Scott J. Kenyon⁷, Marc J. Kuchner⁴

点源でfitできる



Colorが赤く、accretion phase



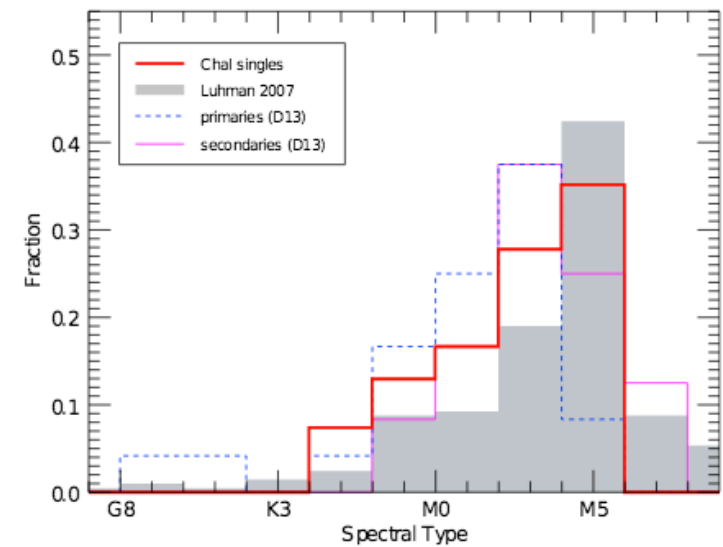
The frequency of accretion disks around single stars: Chamaeleon I

Sebastian Daemgen¹, R. Elliot Meyer¹, Ray Jayawardhana² and Monika G. Petr-Gotzens³

Accepted by A&A

<http://arxiv.org/pdf/1511.05965>

Single starとBinary systemで同じ年齢(2-3 Myr)の54 low-mass starをBr emissionで観測



Single starでのBr γ 検出率は39%

Binaryでd<100AUは2.4-19%

d>100AUではsingleと同等

Accretor fraction は47.8%

→accretion diskがbinaryでは減少

Fig. 1. Spectral type distribution of the Cha I single star sample. For comparison, we also show the overall distribution of Cha I members Luhman (2007) as well as components of binary stars in D13.

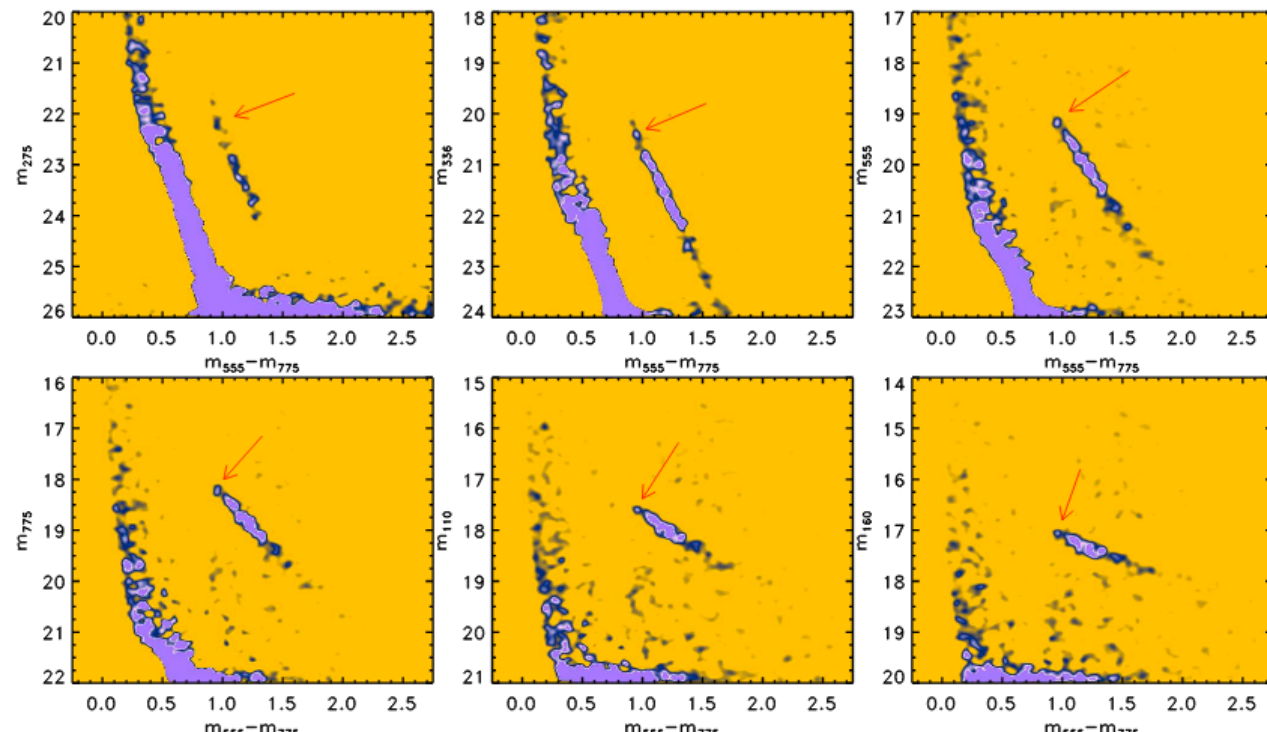
Hubble Tarantula Treasury Project. IV. The extinction law

Guido De Marchi¹, Nino Panagia^{2,3,4}, Elena Sabbi², Daniel Lennon⁵, Jay Anderson², Roelan van der Marel², Michele Cignoni², Eva K. Grebel⁶, Soeren Larsen⁷, Dennis Zaritsky⁸, Peter Zeidler⁶, Dimitrios Gouliermis⁹ and Alessandra Aloisi²

Accepted by MNRAS

<http://arxiv.org/pdf/1510.8436>

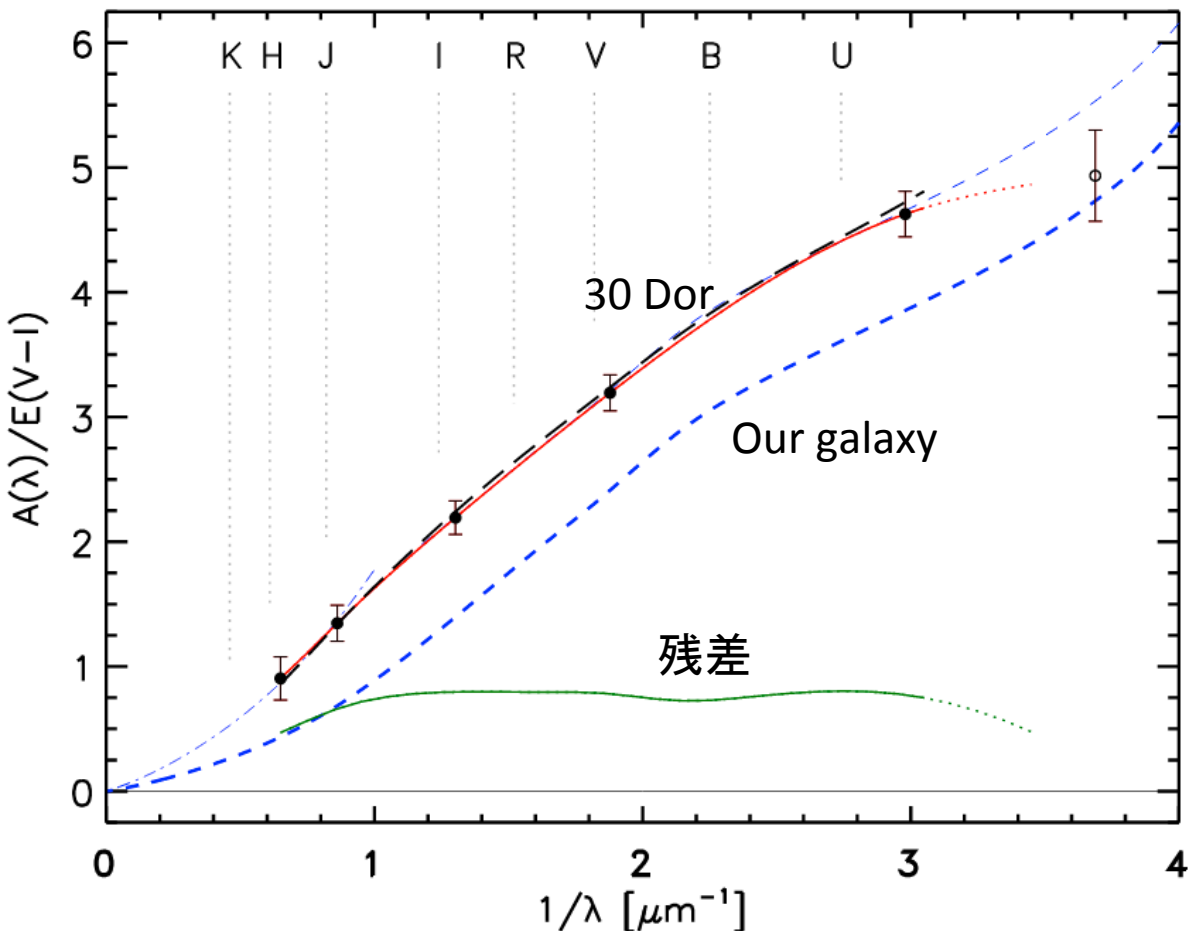
Color magnitude diagram (CMD)を用いて30 Dor in LMCのdust 減光量を見積もった



(1)	(2)	(3)	(4)	(5)	(6)	(7)	(8)	(9)	(10)
Band combination	λ [Å]	$1/\lambda$ [μm^{-1}]	R Whole field	R North	R South	R Northeast	R Northwest	R Southeast	R Southwest
$A_{275}/E(m_{555} - m_{775})$	2 712	3.69	5.15 ± 0.38	5.15 ± 0.49	5.12 ± 0.55	5.07 ± 1.01	4.96 ± 0.86	4.71 ± 0.56	5.11 ± 0.79
$A_{336}/E(m_{555} - m_{775})$	3 356	2.98	4.79 ± 0.19	4.92 ± 0.29	4.69 ± 0.23	5.00 ± 0.38	4.82 ± 0.47	4.55 ± 0.40	4.81 ± 0.38
$A_{555}/E(m_{555} - m_{775})$	5 322	1.88	3.35 ± 0.15	3.44 ± 0.21	3.20 ± 0.19	3.47 ± 0.14	3.41 ± 0.36	3.12 ± 0.32	3.28 ± 0.34
$A_{775}/E(m_{555} - m_{775})$	7 680	1.30	2.26 ± 0.14	2.44 ± 0.19	2.12 ± 0.17	2.47 ± 0.38	2.41 ± 0.31	2.03 ± 0.30	2.20 ± 0.34
$A_{110}/E(m_{555} - m_{775})$	11 608	0.86	1.41 ± 0.15	1.54 ± 0.18	1.26 ± 0.19	1.59 ± 0.33	1.52 ± 0.34	1.23 ± 0.30	1.30 ± 0.43
$A_{160}/E(m_{555} - m_{775})$	15 387	0.65	0.95 ± 0.18	0.98 ± 0.24	0.90 ± 0.22	1.00 ± 0.49	0.98 ± 0.40	0.89 ± 0.33	0.95 ± 0.51

Hubble Tarantula Treasury Project. IV. The extinction law

Guido De Marchi¹, Nino Panagia^{2,3,4}, Elena Sabbi², Daniel Lennon⁵, Jay Anderson², Roelan van der Marel², Michele Cignoni², Eva K. Grebel⁶, Soeren Larsen⁷, Dennis Zaritsky⁸, Peter Zeidler⁶, Dimitrios Gouliermis⁹ and Alessandra Aloisi²



our galaxyと同じdust成分以外に
grey dust(>0.1 um)が存在

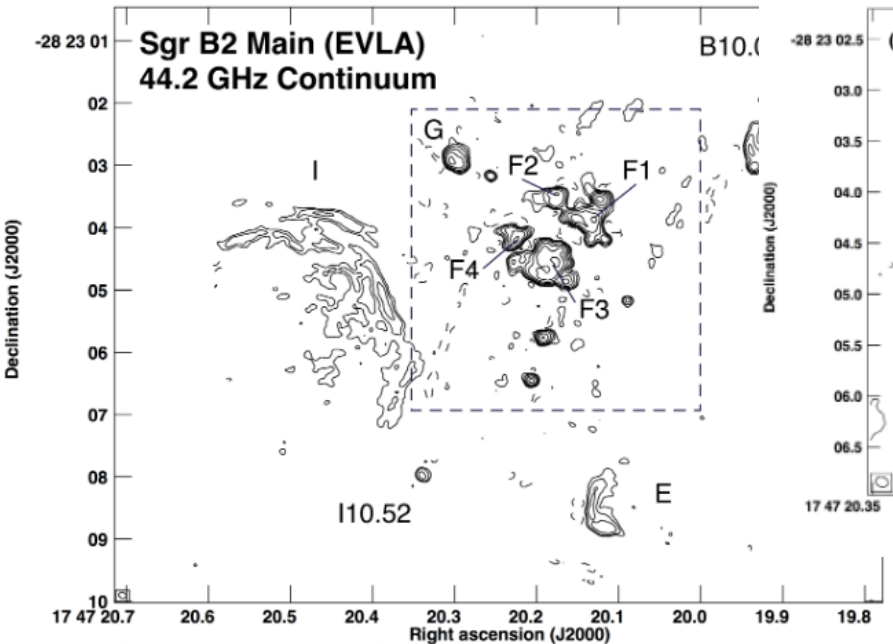
Large scaleで見えているのでtype IIのSneが原因

Evidence of Short Timescale Flux Density Variations of UC H II regions in Sgr B2 Main and North

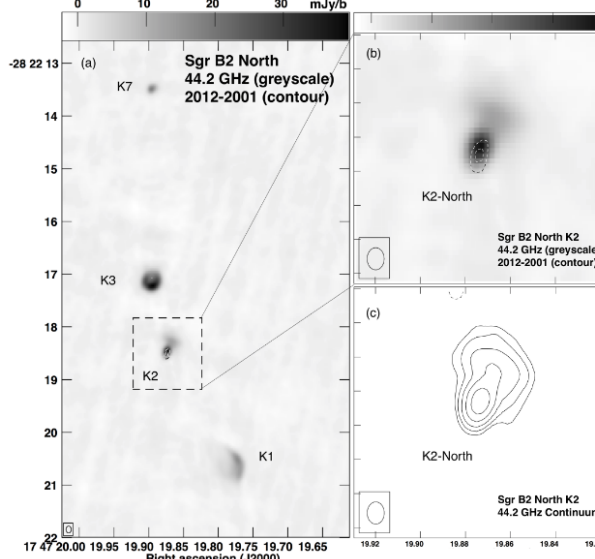
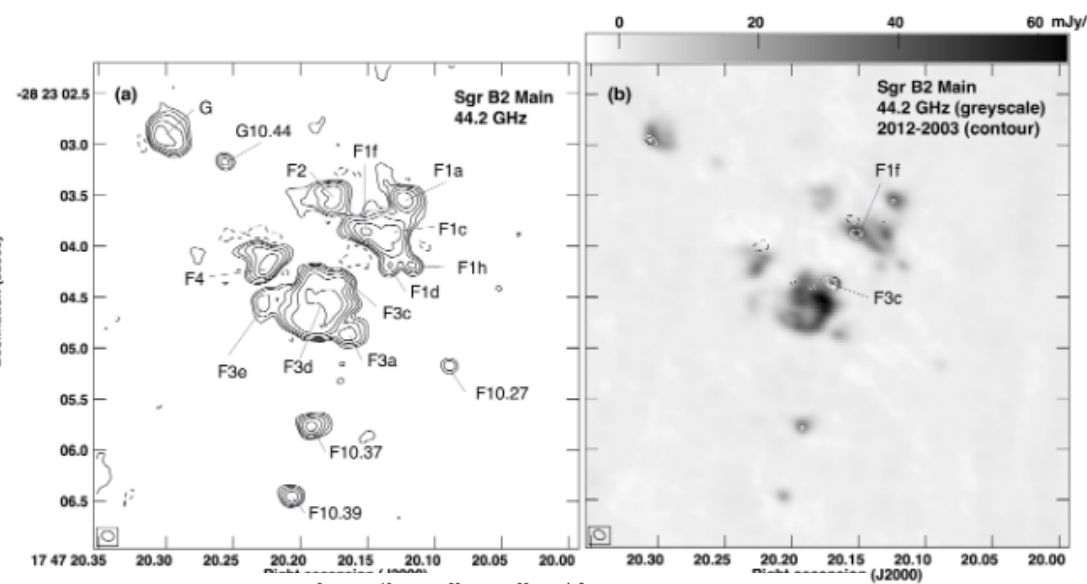
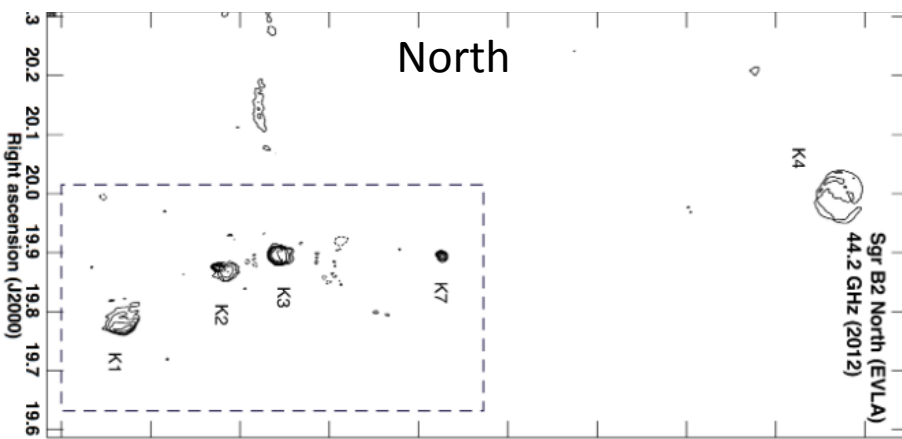
C. G. De Pree¹, T. Peters^{2,3}, M.-M. Mac Low^{4,8}, D. J. Wilner⁵, W. M. Goss⁶, R. Galván-Madrid⁷, E. R. Keto⁵, R. S. Klessen⁸ and A. Monsrud¹

Accepted by The Astrophysical Journal (9 Nov 2015)
<http://arxiv.org/pdf/1511.05131>

Main



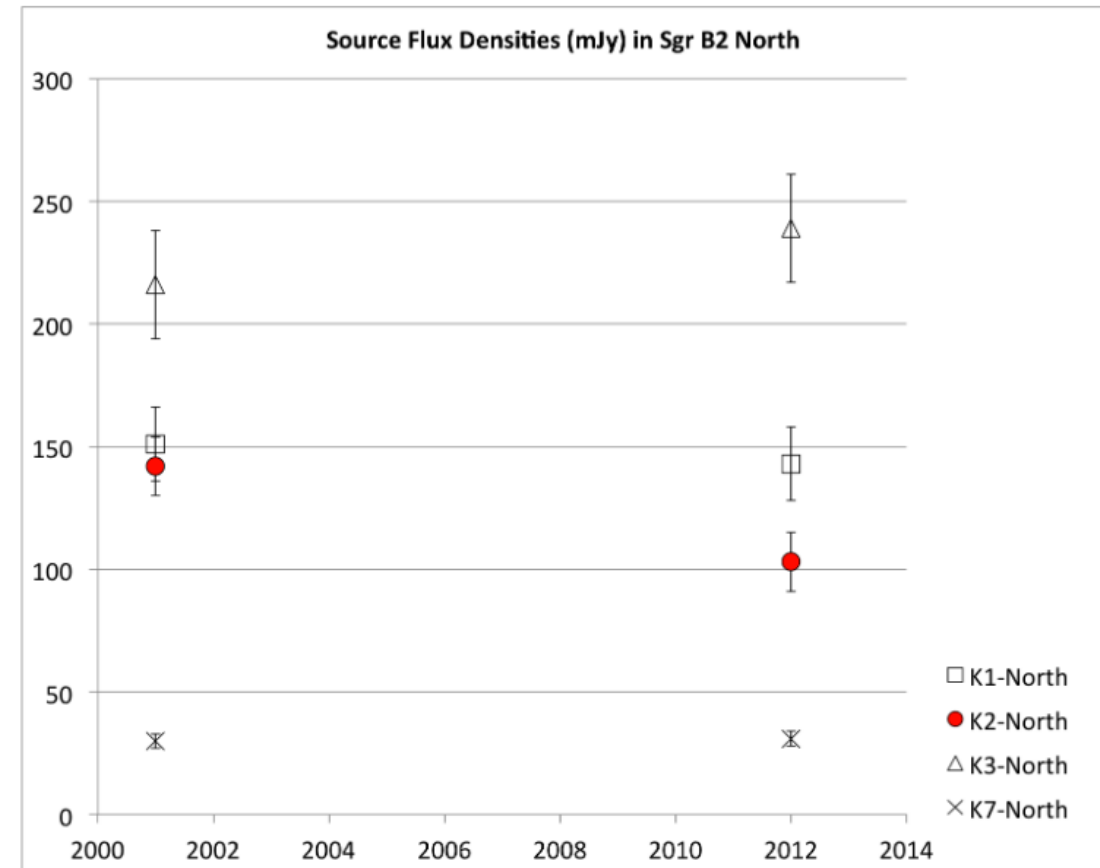
North



Evidence of Short Timescale Flux Density Variations of UC H II regions in Sgr B2 Main and North

C. G. De Pree¹, T. Peters^{2,3}, M.-M. Mac Low^{4,8}, D. J. Wilner⁵, W. M. Goss⁶, R. Galván-Madrid⁷, E. R. Keto⁵, R. S. Klessen⁸ and A. Monsrud¹

12年間で明らかな変動があり、UC H II regionは複雑な構造(球対象でない)をして
短い時間変動のaccretionかionizationをしている



On the effects of rotation in primordial star-forming clouds

Jayanta Dutta^{1,2}

Accepted by A&A

<http://arxiv.org/pdf/1511.00285>

回転するcloudのcollapseをsimulation (SPH, Gadget-2 code) POP III形成

Halo properties	CH1	CH2
n (cm^{-3})	10^6 (max) 71 (min)	10^6 (max) 85 (min)
T (K)	469 (max) 59 (min)	436 (max) 54 (min)
mass (M_\odot)	1030	1093
n -SPH	690855	628773
resolution (M_\odot)	1.3×10^{-2}	1.4×10^{-2}
β_0	0.035 (max) 0.025 (min)	0.042 (max) 0.03 (min)

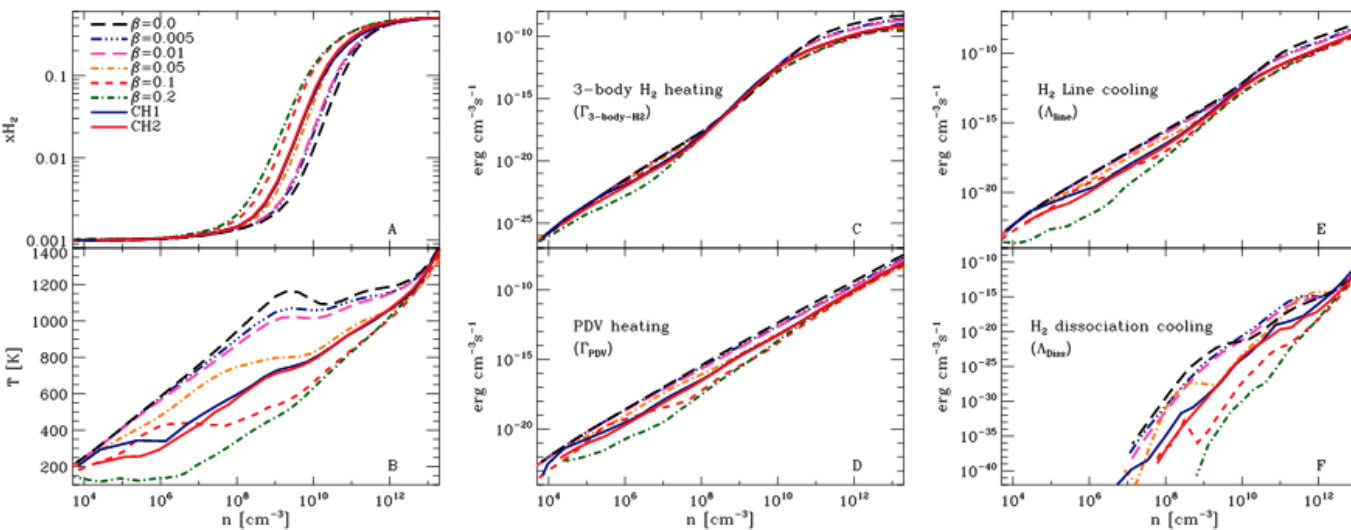
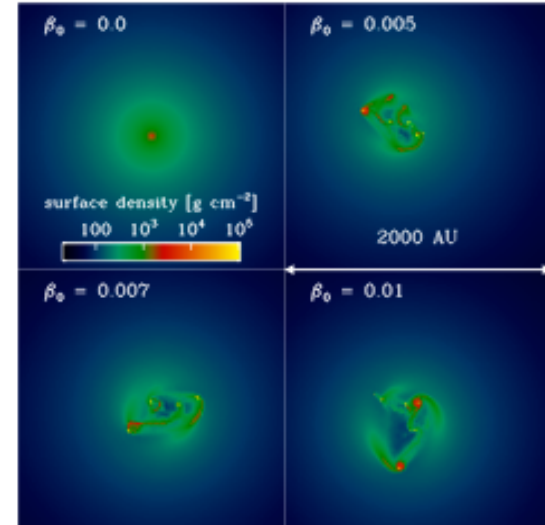
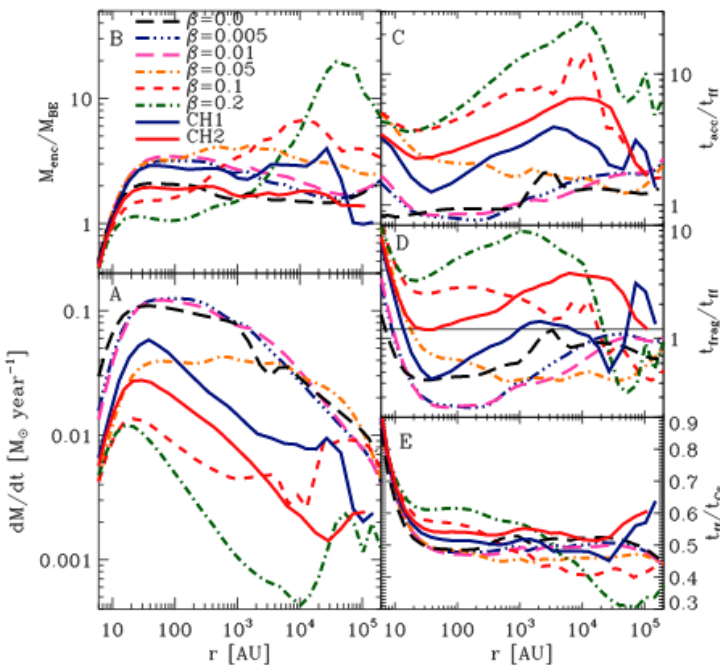
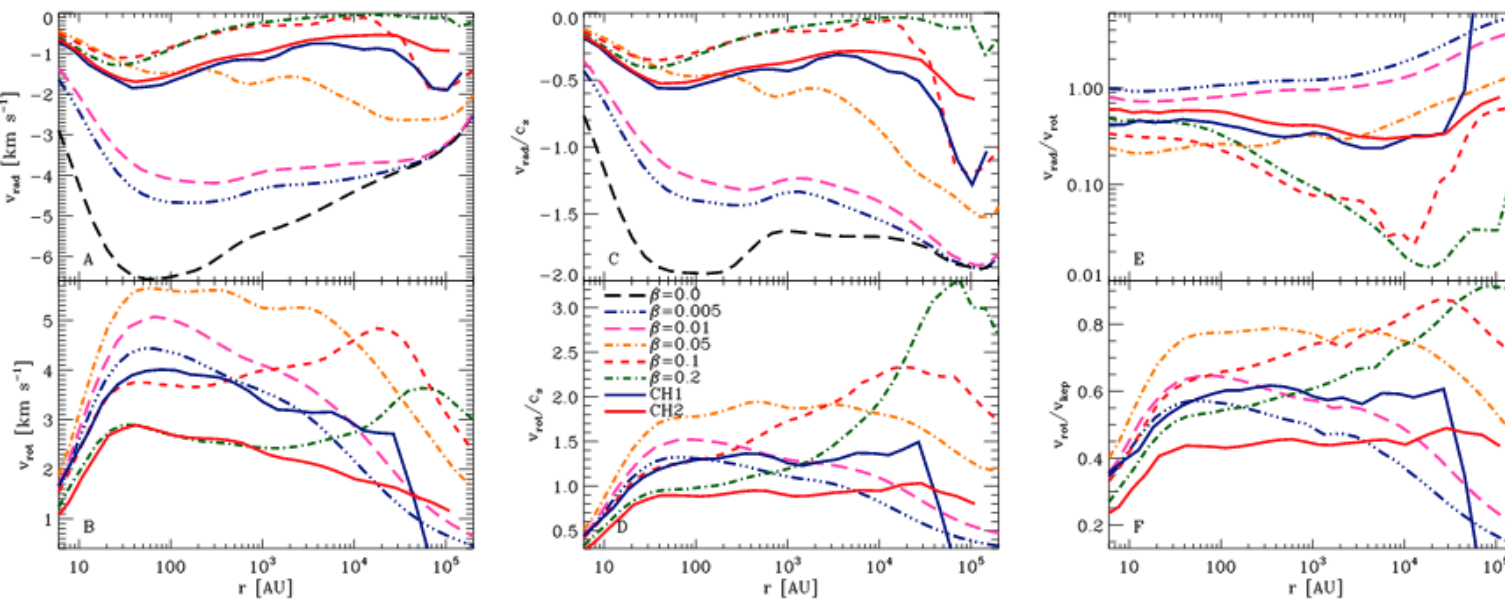


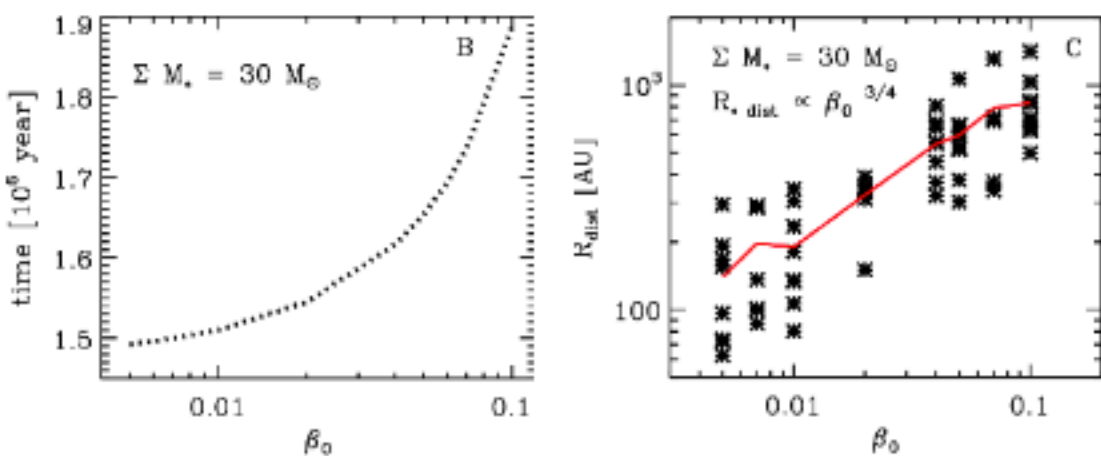
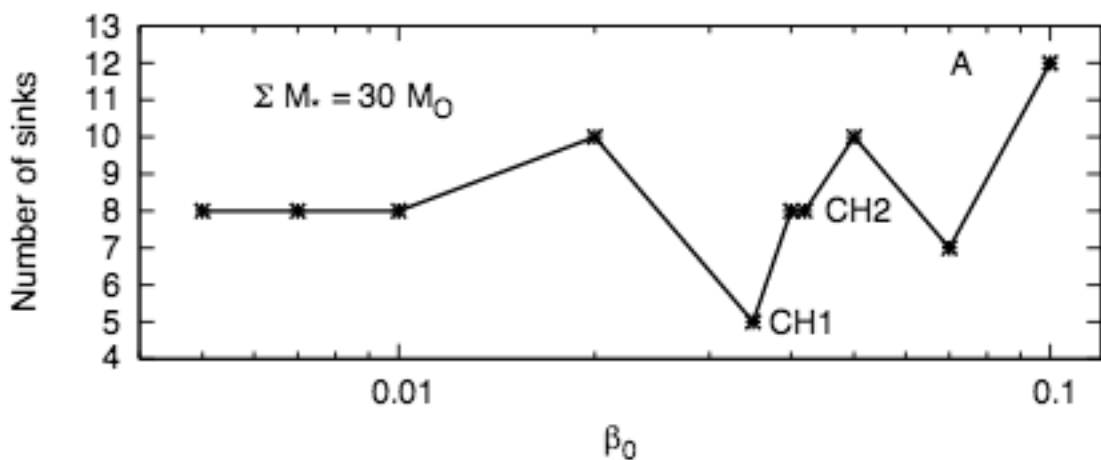
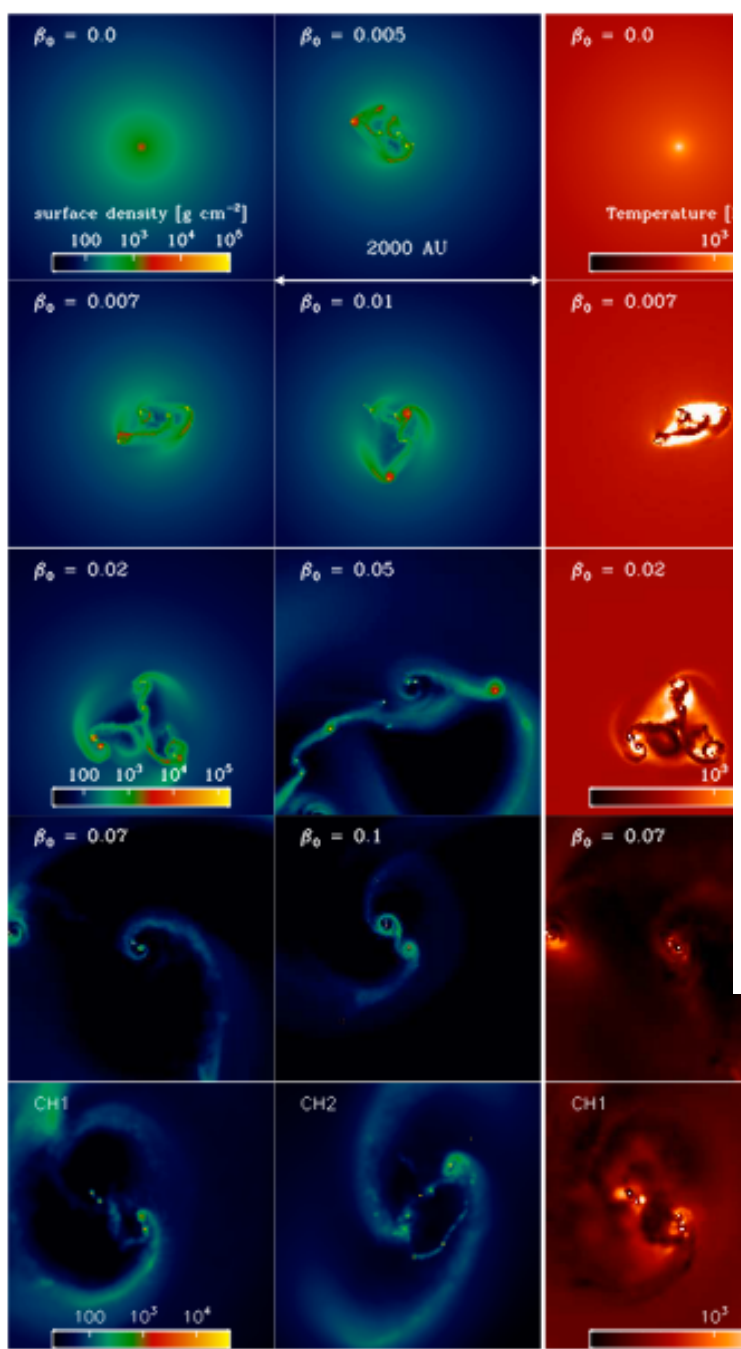
Fig. 1. Radial logarithmic binned, mass-weighted averages of the H_2 fraction (A), temperature (B), and various heating and cooling rates (C to F) are plotted as a function of density for different degrees of initial rotation β_0 , just before the formation of the first sink.

H_2 のfractionは回転によらないが、温度はcompressional heatingの寄与で大きく違う
 H_2 dissociation cooling も同様

回転がないほど v_{rad} は大きく音速程度, $\beta=0.2$ で 10^5 AUではほぼkeplarianでdiskを形成



外側で不安定になりdiskからfragment



回転が大きいとfragmentし、
距離も遠くなる

Fig. 4. The column density and column-weighted temperature distribution in a region of 2000 AU centered around the first protostar for different strengths of the initial rotation of the cloud are shown when a total of $\sim 30 M_\odot$ have been converted into, or accreted onto, sink particles.